

This work is on a Creative Commons Attribution 4.0 International (CC BY 4.0) license, <https://creativecommons.org/licenses/by/4.0/>. Access to this work was provided by the University of Maryland, Baltimore County (UMBC) ScholarWorks@UMBC digital repository on the Maryland Shared Open Access (MD-SOAR) platform.

Please provide feedback

Please support the ScholarWorks@UMBC repository by emailing scholarworks-group@umbc.edu and telling us what having access to this work means to you and why it's important to you. Thank you.

Refactoring Ehrlich Pathway for High-Yield 2-Phenylethanol Production in *Yarrowia lipolytica*

Yang Gu, Jingbo Ma, Yonglian Zhu, and Peng Xu*



Cite This: *ACS Synth. Biol.* 2020, 9, 623–633



Read Online

ACCESS |



Metrics & More



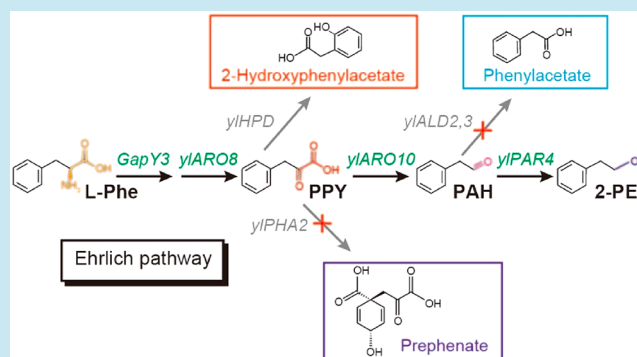
Article Recommendations



Supporting Information

ABSTRACT: Efficient microbial synthesis of chemicals requires the coordinated supply of precursors and cofactors to maintain cell growth and product formation. Substrates with different entry points into the metabolic network have different energetic and redox statuses. Generally, substrate cofeeding could bypass the lengthy and highly regulated native metabolism and facilitates high carbon conversion rate. Aiming to efficiently synthesize the high-value rose-smell 2-phenylethanol (2-PE) in *Y. lipolytica*, we analyzed the stoichiometric constraints of the Ehrlich pathway and identified that the selectivity of the Ehrlich pathway and the availability of 2-oxoglutarate are the rate-limiting factors. Stepwise refactoring of the Ehrlich pathway led us to identify the optimal catalytic modules consisting of L-phenylalanine permease, ketoacid aminotransferase, phenylpyruvate decarboxylase, phenylacetaldehyde reductase, and alcohol dehydrogenase. On the other hand, mitochondrial compartmentalization of 2-oxoglutarate inherently creates a bottleneck for efficient assimilation of L-phenylalanine, which limits 2-PE production. To improve 2-oxoglutarate (αKG) trafficking across the mitochondria membrane, we constructed a cytosolic αKG source pathway by coupling a bacterial aconitase with a native isocitrate dehydrogenase (yIIPD2). Additionally, we also engineered dicarboxylic acid transporters to further improve the 2-oxoglutarate availability. Furthermore, by blocking the precursor-competing pathways and mitigating fatty acid synthesis, the engineered strain produced 2669.54 mg/L of 2-PE in shake flasks, a 4.16-fold increase over the starting strain. The carbon conversion yield reaches 0.702 g/g from L-phenylalanine, 95.0% of the theoretical maximal. The reported work expands our ability to harness the Ehrlich pathway for production of high-value aromatics in oleaginous yeast species.

KEYWORDS: stoichiometric model, *Yarrowia lipolytica*, cofactor engineering, 2-phenylethanol, pathway selectivity, Ehrlich pathway



Metabolic engineering is the enabling technology to rewire cellular endogenous metabolism for the optimal production of native metabolites, or endow cells with the capacity for synthesizing nonnative chemicals.¹ To date, there are numerous studies of engineering microbes for production of commodity chemicals and natural products, including the production of cannabinoids,² artemisinin,³ taxol precursors,^{4,5} branched-chain alcohols,^{6,7} ornithine,⁸ arginine,⁹ advanced biofuels,^{10–13} and so on, from different host organisms. The primary goal of metabolic engineers is to achieve high titer, yield, and productivity (TYP) with improved cost-efficiency and process economics.^{14,15} In the past decades, a number of prominent metabolic engineering strategies and methodologies have been adopted to balance or redirect metabolic flux, such as modular pathway engineering,¹⁰ dynamic pathway regulation,^{16–19} cofactor engineering,^{20,21} and scaffold-guided spatial colocalization of metabolic enzymes,^{22,23} *et al.* The spatiotemporal or ratiometric control of enzyme expression have been proven as efficient strategies to relieve metabolic burden and improve the TYP index.

However, the complex and lengthy synthetic routes from the starting carbons, such as glucose, commonly generate low yield and suboptimal productivity of desired products, which could be attributed to that complex biosynthesis requires the coordinated supply of precursors, ATPs, and reducing equivalents (NADPH/NADH) to maintain both cell metabolism and product formation.^{24,25} Substrates with different entry points into the metabolic network have different energetic and redox statuses,^{24,26} which leads to pathway-dependent product yields that critically affect cost-efficiency. Thus, providing microbes with multiple carbon sources can potentially mitigate these metabolic constraints, since it adds an additional degree of freedom to cellular systems that can be

Received: November 19, 2019

Published: March 5, 2020

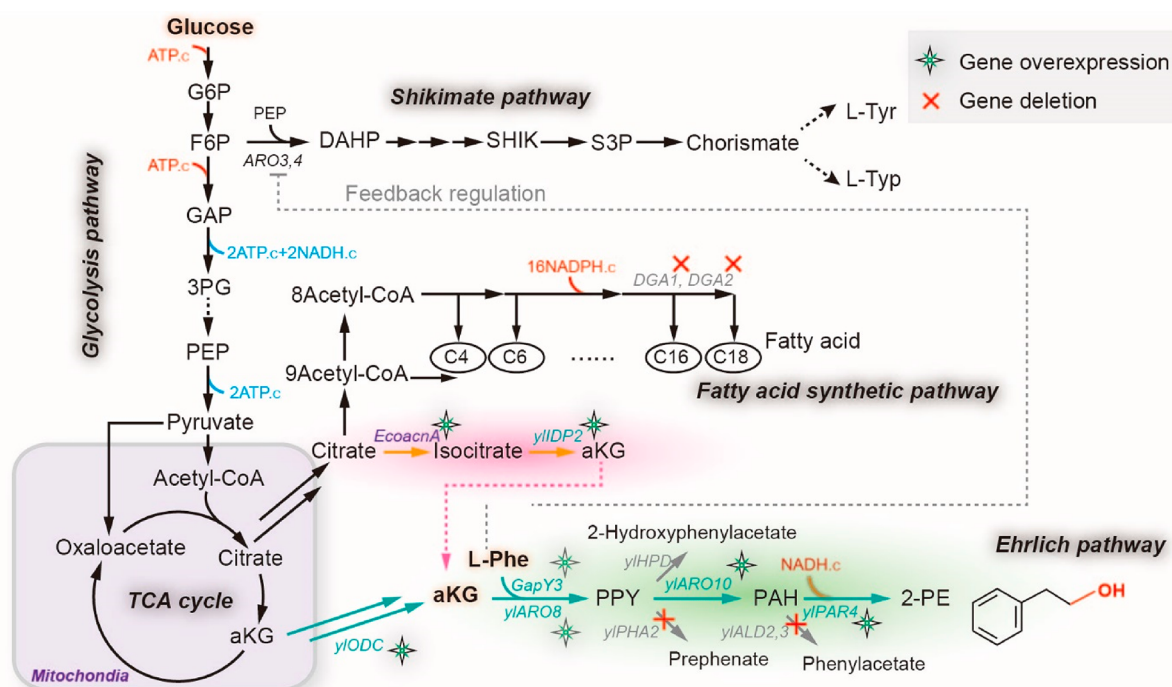


Figure 1. Central carbon metabolism and Ehrlich pathway for synthesizing 2-PE in *Y. lipolytica*. L-Phe, L-phenylalanine; PPY, phenylpyruvate; PAH, phenylacetaldehyde; *GapY3*, L-phenylalanine specific permease; *yLARO8*, L-phenylalanine transaminases; *yLHPD*, 4-hydroxyphenylpyruvate dioxygenase; *yIPHA2*, prephenate dehydratase; *yLARO10*, phenylpyruvate decarboxylase; *yIPAR4*, phenylacetaldehyde reductases; *ALD2,3*, aldehyde dehydrogenase; G6P, glucose-6-phosphate; F6P, fructose 6-phosphate; GAP, glyceraldehyde-3-phosphate; 3PG, 3-phospho-glycerate; PEP, phosphoenolpyruvate; aKG, 2-oxoglutarate; DAHP, 3-deoxy-arabino-heptulonate-7-phosphate; SHIK, shikimate; S3P, shikimate-3-phosphate; L-Tyr, L-tyrosine; L-Typ, L-tryptophan; *ARO3,4*, 3-deoxy-7-phosphoheptulonate synthase; *yIODC*, 2-oxodicarboxylate carrier; *yIDP2*, cytosolic isocitrate dehydrogenase; *EcoacnA*, aconitate hydratases; *DGA1,2*, diacylglycerol acyltransferase;

leveraged for product formation (namely, cosubstrate feeding).²⁶ One recent example is to use the acetate-driven acetyl-CoA metabolic shortcut to bypass the lengthy and highly regulated glycolytic pathway for efficient polyketides²⁷ and lipids production.²⁴ Such substrate doping strategy may present a metabolic advantage over a single substrate and lead to metabolic optimality beyond what can be achieved in single substrate fermentations. In other words, single substrate strategies may not be suitable for particular metabolic engineering applications. Instead, metabolite doping or cosubstrate feeding can overcome intrinsic pathway limitations and achieve high carbon conversion efficiency and cost-efficiency.

2-Phenylethanol (2-PE) is a high-value compound widely used in the food, fragrance, and flavor industries. High-quality 2-PE is primarily extracted from the volatile oil components of rose flower, with a marketed price ranging from \$150/kg to \$200/kg, which suffers from economics and scalability issues for sustainable production.²⁸ Chemically synthesized 2-PE, despite its low-cost and high conversion rate, is largely rejected by consumers and IFF society (International Flavors & Fragrances) due to safety and health issues.²⁹ As a result, heterologous production of 2-PE from microbial host is considered as an economically viable alternative to plant extraction. Herein, *Yarrowia lipolytica* was chosen as the host strain because of its strong acetyl-CoA flux and high TCA metabolic activity and the ease of genetic toolbox,³⁰ as demonstrated by its superior performance for production of advanced biofuels and oleochemicals.³¹ In addition, *Y. lipolytica* is also a "Generally Regarded As Safe" (GRAS) organism in the food and nutraceutical industry.³²

To demonstrate the utility of substrate cofeeding, we harnessed the Ehrlich pathway of *Yarrowia lipolytica* to optimize the biosynthesis of 2-phenylethanol (2-PE), with glucose and L-phenylalanine as the cosubstrates. The bioconversion process involves deamination, decarboxylation, and aldehyde reduction (Figure 1), with several aromatic byproducts branched out from this pathway (Figure 1). In particular, the deamination is an α -ketoglutarate (aKG)-coupled amino transfer reaction and aldehyde reduction is a NADH-dependent reduction reaction (Figure 1). Both the aKG and NADH, as cofactors, are derived from glucose. To improve the precursor flux and maximize 2-PE production, we have applied a stoichiometric model to determine the pathway yield and predict engineering targets (Supplementary Note). To improve the overall pathway specificity, we characterized and reconfigured all the biochemical reactions in Ehrlich pathway by stepwise pathway refactoring more than 20 enzymes, and further blocked the competing pathways to eliminate any byproducts. On the other hand, cytosolic 2-oxoglutarate (aKG) is the cofactor to complete the amine transfer reaction. But aKG is derived from the oxidative decarboxylation of isocitrate that is primarily compartmentalized in mitochondria, creating a bottleneck for efficient assimilation of L-Phe, which limits 2-PE production. To improve metabolite trafficking across the mitochondria membrane, we constructed an artificial aKG source pathway in the cytosol, by coupling a cytosolic aconitase with the overflowed citrate from mitochondria. In addition, we further improved the aKG supply and 2-PE production by mitigating fatty acid synthesis. As a result, the engineered strain (**po1fk7P**) produced 2669.54 mg/L of 2-PE with 0.702 g/g

conversion yield from L-Phe, representing about 4.16-fold and 2.07-fold increase over the starting strain (641.59 mg/L of 2-PE production with 0.339 g/g_{L-phenylalanine}), respectively. Taken together, refactoring critical enzymes and increasing metabolite trafficking as well as mitigating competitive pathways are effective strategies to improve the efficiency of overall pathway yield.

RESULTS AND DISCUSSION

Characterization of Ehrlich Pathway for 2-PE Synthesis in *Y. lipolytica*. Microbially produced 2-PE is mainly obtained by two routes, namely, the *de novo* pathway from glucose and bioconversion from L-phenylalanine by the Ehrlich pathway. Owing to the hard-wired, tightly complex feedback regulation³³ and lengthy reaction steps (>20 steps) of the *de novo* pathway, bioconversion by the Ehrlich pathway is considered as the preferred biological route to synthesize 2-PE.²⁸ In the Ehrlich pathway (Figure 1), L-phenylalanine is converted to 2-PE through four enzyme-dependent processes: (i) extracellular L-phenylalanine is internalized by amino permeases; (ii) L-phenylalanine is transaminated to phenylpyruvate by amino transferase with 2-oxoglutarate (aKG) as the amine-receptor; (iii) phenylpyruvate is further decarboxylated to phenylacetaldehyde by phenylpyruvate decarboxylases; (iv) and finally, phenylacetaldehyde is reduced to 2-PE by alcohol dehydrogenases or phenylacetaldehyde reductase with NADH as cofactor.

In *Y. lipolytica*, transaminases and the phenylpyruvate decarboxylase are yARO8 (encoded by gene YALI0E20977g) or yARO9 (encoded by gene YALI0C05258g) and yARO10 (encoded by gene YALI0D06930g), respectively. However, the specific L-phenylalanine permease and phenylacetaldehyde alcohol dehydrogenases have not been characterized. To determine the ability of *Y. lipolytica* in producing 2-PE, *Y. lipolytica* po1g (leu⁻) harboring an empty plasmid pYXLP' (strain po1g pYXLP') was used as control to incubate with different concentrations of L-phenylalanine (0, 2, 4, 6, 8, and 10 g/L) in shake flasks. Our results (Figure 2a) indicate that the highest titer of 2-PE reached 720.43 mg/L with 0.342 g/g_{L-phenylalanine} yield by adding 10 g/L L-phenylalanine, accompanying with 197.59 mg/L of byproduct phenylacetate. Considering economic efficiency (incomplete conversion of L-Phe), 4 g/L of L-phe was able to support 641.59 mg/L (Figure 2b) of 2-PE production with 0.339 g/g_{L-phenylalanine} yield (Figure 2c). Thus, in the following work, 4 g/L of L-phe was determined for bioconversion.

Refactoring the Upstream Ehrlich Pathway to Improve 2-PE Yield. As suggested by the mathematical model (Supplementary Note S1), improving the catalytic efficiency of the Ehrlich pathway and increasing aKG supplementation are the key determinants to improve 2-PE yield from L-phenylalanine. To refactor the Ehrlich pathway, we adopted a stepwise pathway engineering strategy. First, the native yARO8, yARO9, and yARO10 genes in Ehrlich pathway were overexpressed in *Y. lipolytica* po1g under the control of strong constitutive TEF-intron promoter. Shaking flask cultivation (Figure 2d, and Figure 2e,f for cell growth and 2-PE yield) indicates that overexpression of yARO8 and yARO9 (strain po1gP1 and po1gP2) has little effect on the 2-PE production. However, overexpression of yARO10 (strain po1gP3) increased 2-PE titer to 922.86 mg/L, about 33% higher than the control strain (Figure 2d), suggesting that the reaction catalyzed by phenylpyruvate decarboxylase yARO10

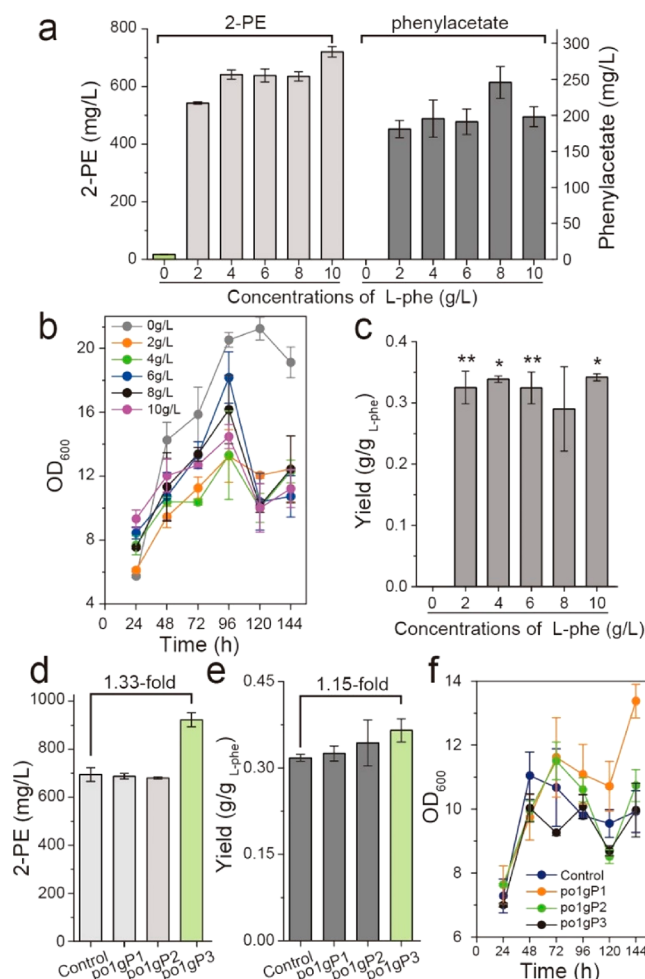
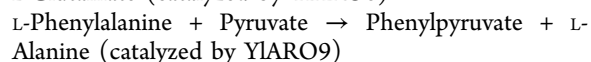
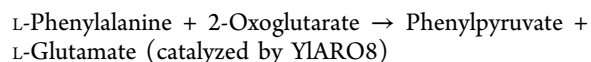


Figure 2. Initial assessment of using *Y. lipolytica* to produce 2-PE from L-phenylalanine via the Ehrlich pathway. (a–c) 2-PE and phenylacetate titer, time profiles of cell growth, and 2-PE yield of adding different concentrations L-phenylalanine (0, 2, 4, 6, 8, and 10 g/L). (d–f) 2-PE titer, yield, and cell growth of respective overexpressing genes yARO8, yARO9, and yARO10. All experiments were performed in triplicate and error bars show standard deviation (SD). The * indicates $p < 0.01$, and ** indicates $p < 0.05$ (two-tailed test).

is a limiting-step in Ehrlich pathway. Thus, the ineffectiveness of overexpressing downstream genes (yARO8 or yARO9) is likely due to the limited performance of the upstream yARO10. Specifically, yARO8 and yARO9 are both transaminases, which catalyze the transamination of L-phenylalanine with different amine-receptors:



Apparently, different amine-receptors (that is 2-oxoglutarate and pyruvate) will lead to distinct outcomes (that is L-glutamate and L-alanine) that may affect 2-PE production. Therefore, we next constructed strains carrying pYXLP'-yARO10-yARO8 and pYXLP'-yARO10-yARO9 to identify the optimal transaminases, and obtained po1gP4 and po1gP5. However, screening of these two strains showed no significant differences in 2-PE production (Figure 3b, and Figure 3c,d for cell growth and 2-PE yield). We also overexpressed a

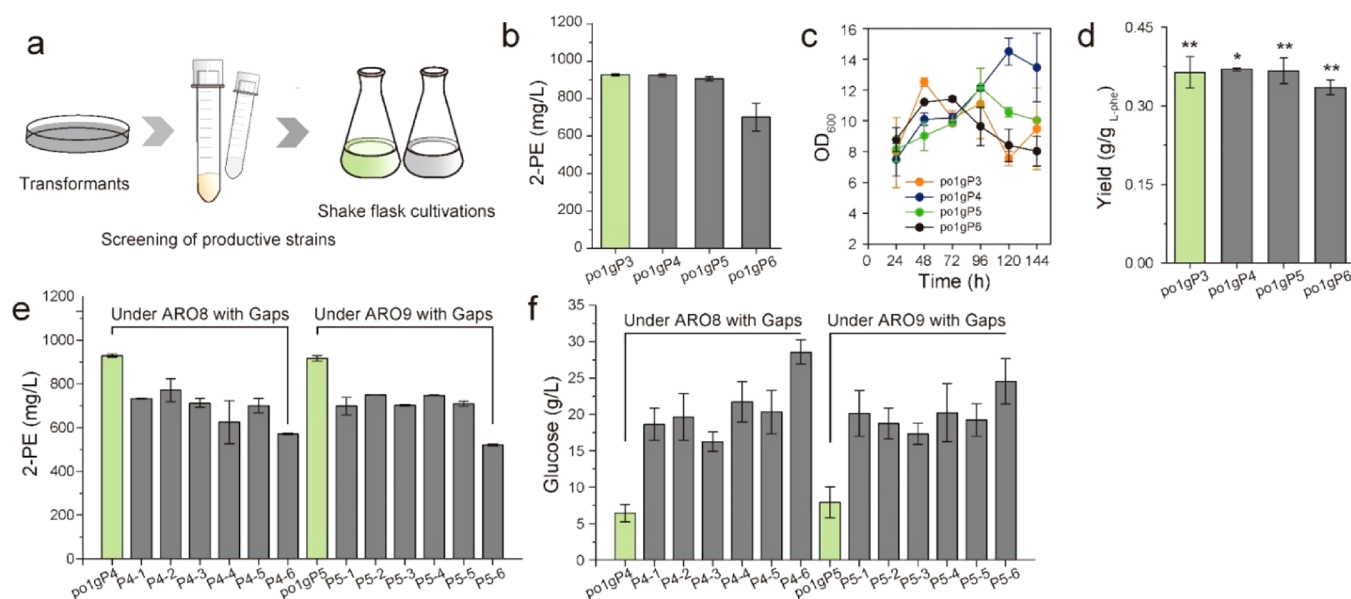


Figure 3. Characterization of upstream module of the Ehrlich pathway: L-phenylalanine specific permeases and L-phe: 2-oxoglutarate transaminase. (a) Flow-chart of shake flask cultivations of engineered strains. (b–d) 2-PE titers, cell growth, and 2-PE yield of respective overexpressing genes *yLARO10* and *yLARO8*, *yLARO10* and *yLARO9*, and *yLARO10* and *C18645*. (e,f) 2-PE titers and 96h residual glucose of screening L-phenylalanine specific permeases with CSM fermentation medium in shake cultivations. All experiments were performed in triplicate and error bars show standard deviation (SD). The * indicates $p < 0.01$, and ** indicates $p < 0.05$ (two-tailed test).

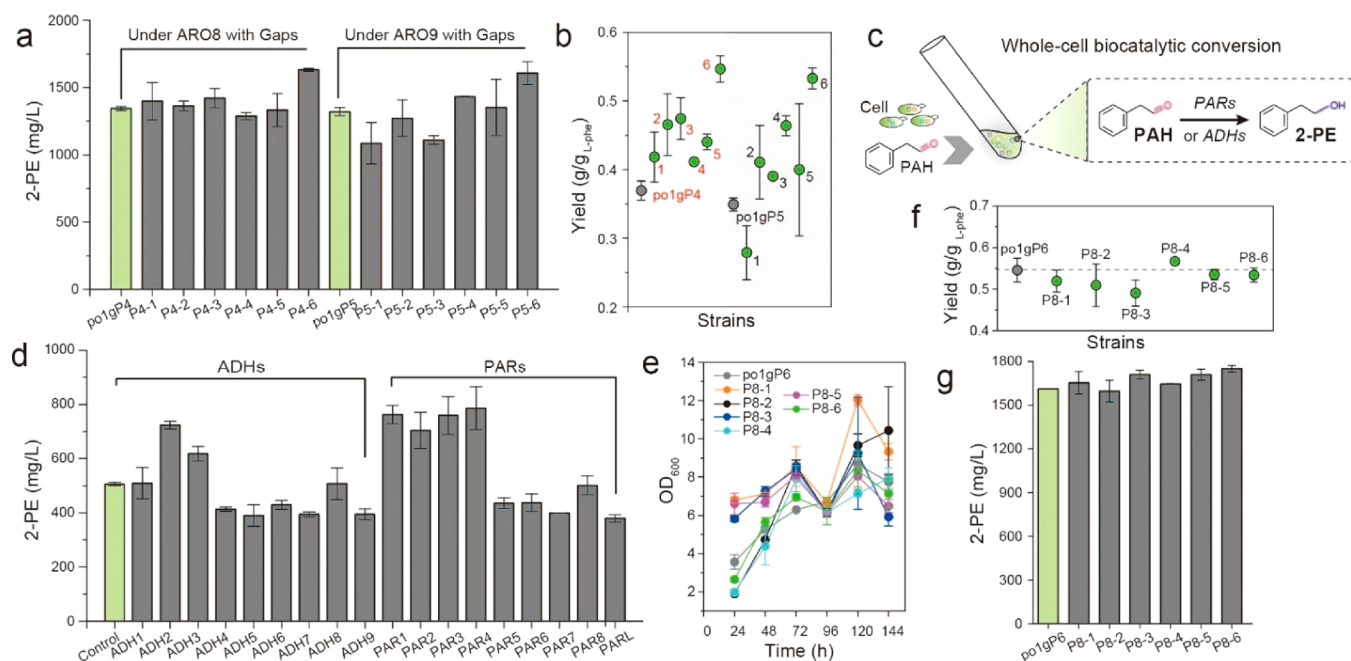


Figure 4. Characterization of the downstream module of the Ehrlich pathway: phenylacetaldehyde reductases and alcohol dehydrogenases. (a,b) 2-PE titers and yield by rescreening L-phenylalanine specific permeases. Red 1, strain P4-1; Red 2, strain P4-2; Red 3, strain P4-3; Red 4, strain P4-4; Red 5, strain P4-5; Red 6, strain P4-6; Black 1, strain P5-1; Black 2, strain P5-2; Black 3, strain P5-3; Black 4, strain P5-4; Black 5, strain P5-5; Black 6, strain P5-6. (c) Manipulations of whole-cell biocatalytic conversion of phenylacetaldehyde. PAH, phenylacetaldehyde. (d–g) 2-PE titers, cell growth and yield of screening and identifying the optimized phenylacetaldehyde reductases or alcohol dehydrogenases. P8-1, strain po1gP8-1; P8-2, strain po1gP8-2; P8-3, strain po1gP8-3; P8-4, strain po1gP8-4; P8-5, strain po1gP8-5; P8-6, strain po1gP8-6. All experiments were performed in triplicate and error bars show standard deviation (SD).

transcriptional activator (encoded by *YALI0C18645*) to up-regulate the expression of *yLARO8* or *yLARO9*.²⁹ However, cultivation of this strain (po1gP6) showed deteriorated 2-PE production (Figure 3b). With this, we speculated that cellular uptake of L-phe might be the bottleneck limiting 2-PE titer.

To facilitate the cellular uptake for L-phe, we assessed a number of L-phe permease, including BAP and Gap1 from *S. cerevisiae*,³⁴ PheP from *E. coli*, and three *Y. lipolytica* native Gap1 homologues, encoded by *YALI0C17237g* (named as *GapY1*), *YALI0B16522g* (*GapY2*), and *YALI0B19800g* (*GapY3*), respectively. Beyond our expectation, all the tested

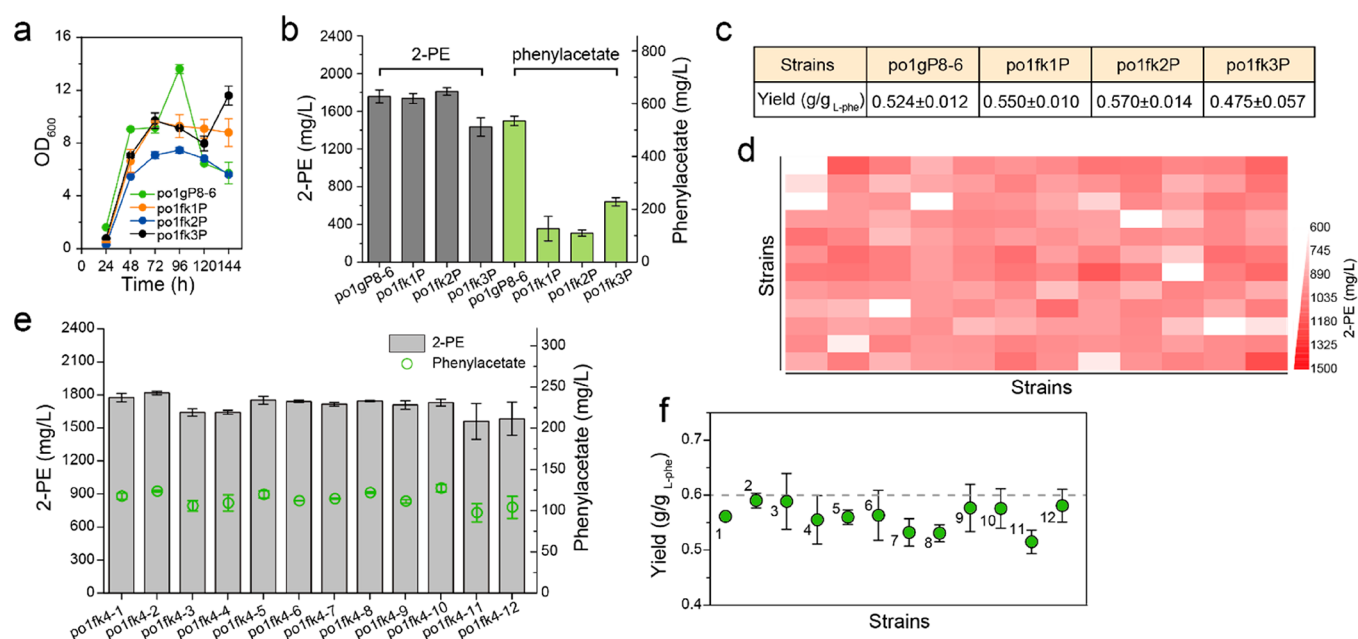


Figure 5. Blocking competitive pathways and integration of the Ehrlich pathway in 26s rDNA sites to improve 2-PE production. (a–c) Cell growth, 2-PE titers, phenylacetate titers, and 2-PE yield of blocking competitive pathways. (d) Screening of the productive strains based on 24-well deep plate cultivations. (e,f) 2-PE titer and yield by further validating productive strains with integration of the Ehrlich pathway in flask cultivations. 1, strain **po1fk4-1**; 2, strain **po1fk4-2**; 3, strain **po1fk4-3**; 4, strain **po1fk4-4**; 5, strain **po1fk4-5**; 6, strain **po1fk4-6**; 7, strain **po1fk4-7**; 8, strain **po1fk4-8**; 9, strain **po1fk4-9**; 10, strain **po1fk4-10**; 11, strain **po1fk4-11**; 12, strain **po1fk4-12**. All experiments were performed in triplicate and error bars show standard deviation (SD).

L-phe permeases showed decreased 2-PE production compared with control **po1gP4** and **po1gP5** when coupling with expression of *ylARO8-ylARO10* or *ylARO9-ylARO10* (Figure 3e). Noticeably, abundant residual glucose was detected at 96 h (Figure 3f), suggesting the central carbon metabolism of these strains was strongly inhibited. This result is consistent with the finding that high level of endogenous *L*-phe induces a strong down regulation of cellular metabolism in *S. cerevisiae*.³⁵ We reasoned that a similar effect might exist in *Y. lipolytica*. Thus, we dropped out all other amino acids and only used YNB-glucose with 4 g/L *L*-phe as the nitrogen source. As a result, the highest 2-PE titer reached 1632.73 mg/L with 0.547 g/g_{*L*-phenylalanine} yield in strain **po1gP4-6** (Figure 4a,b) after 144 h cultivation, indicating GapY3 is a potent *L*-phe permease. Nevertheless, differences of 2-PE titers in strains **po1gP4-6** and **po1gP5-6** (1607.46 mg/L with 0.533 g/g_{*L*-phenylalanine}) were insignificant, which may be attributed to the poor substrate specificity of transaminases *ylARO8* and *ylARO9*.

Refactoring the Downstream Ehrlich Pathway to Improve 2-PE Yield. To refactor the optimal alcohol dehydrogenase (ADH) or phenylacetaldehyde reductase (PAR), we screened the entire genome of *Y. lipolytica* with putative rose phenylacetaldehyde reductase PARL as the template, and identified eight PARs with high similarity (>70%), encoded by *YALIO08844g* (PAR1), *YALIOF09097g* (PAR2), *YALIOF24937g* (PAR3), *YALIO07062g* (PAR4), *YALIO12386g* (PAR5), *YALIOC20251g* (PAR6), *YALIO11616g* (PAR7), and *YALIO08778g* (PAR8), respectively. We also codon-optimized and synthesized the rose-derived PARL as a positive control. The resulting 9 strains, with overexpression of PAR1, PAR2, PAR3, PAR4, PAR5, PAR6, PAR7, PAR8, and PARL, were incubated with 1 g/L phenylacetaldehyde (Figure 4c), leading to 2-PE titers of 762.71, 703.62, 759.37, 786.58, 435.61, 437.33, 399.11, 501.10,

and 379.28 mg/L (Figure 4d), respectively. The highest 2-PE titer was produced by strain **PAR4** (*YALIO07062g*). Interestingly, the rose-derived PARL performed worst in our test.

Similarly, we also investigated the performances of alcohol dehydrogenases (ADHs) in *Y. lipolytica*. Nine *Y. lipolytica* ADHs annotated by Genbank (<https://www.ncbi.nlm.nih.gov/genbank/>) and GRYC (<http://gryc.inra.fr/>) were tested, including ADH1 (*YALIO025630g*), ADH2 (*YALIOE17787g*), ADH3 (*YALIOA16379g*), ADH4 (*YALIOA15147g*), ADH5 (*YALIOE07766g*), ADH6 (*YALIOE15818g*), ADH7 (*YALIO02167g*), ADH8 (*YALII1C17782g*), and ADH9 (*SFA1*). The resulting strains were tested and only suboptimal level of 2-PE were detected in these strains compared to the strain harboring the optimal PARs (Figure 4d), and the best strain (ADH2) produced 723.74 mg/L 2-PE, which is about 10% lower than strain **PAR4**.

After analyzing the downstream PAR and ADH modules, we chose six efficient candidates for further investigation, including ADH2, ADH3, PAR1, PAR2, PAR3, and PAR4. These PARs and ADHs were combined with the optimal upstream module *ylARO10-ylARO8-GapY3*, leading to strains **po1gP7-1**, **po1gP7-2**, **po1gP7-3**, **po1gP7-4**, **po1gP7-5**, and **po1gP7-6**. When tested in shake flask with YNB-glucose media and 4 g/L *L*-phenylalanine, these strains produced 2-PE at 1126.62, 902.12, 1109.89, 1166.23, 960.96, and 1378.98 mg/L, respectively (Supplementary Figure S3), representing no improvements in 2-PE titer compared to control **po1gP4-6** (*ylARO10-ylARO8-GapY3*, 1610.76 mg/L). We speculated that simultaneous overexpression of four genes (>16 000 bp) may lead to genetic instability (loss of plasmid or unequal distribution/propagation of plasmid) in *Y. lipolytica*. To test this hypothesis, we linearized these plasmids and integrated the long DNA cassettes at the pBR docking site of **po1g**

chromosome, leading to strains **polgP8-1**, **polgP8-2**, **polgP8-3**, **polgP8-4**, **polgP8-5**, and **polgP8-6**, respectively. Shake flask screening indicates that **polgP8-6** produced 1750.46 mg/L of 2-PE with 0.534 g/g yield (Figure 4f,g, and Figure 4e for cell growth), the highest titer obtained, indicating PAR4 is the optimal downstream module that reduces phenylacetaldehyde to 2-PE. So far, the four steps of the Ehrlich pathway (permeation, transamination, decarboxylation, and reduction) have been fully refactored, and the refactored pathway represents 2.4-fold increase in 2-PE titer over the starting strain (~710 mg/L).

Blocking Competing Pathways to Improve 2-PE Titer.

To further improve 2-PE yield, we attempted to delete the competing pathways. For the convenience of the genetic manipulations, we first knocked out gene *ku70* in **pol1f** (named **pol1fk**) to inhibit nonhomologous end joining (NHEJ) and improve the frequency of homologous recombination.

As mentioned above, the major byproduct is phenylacetate, which is the oxidized product of phenylacetaldehyde catalyzed by aldehyde dehydrogenases (ALD2 and ALD3). Thus, we sequentially knocked out both *ALD2* (*YALI0D07942g*) and *ALD3* (*YALI0F04444g*) in **pol1fk**, obtaining strain **pol1fk1**. Then the optimal upstream and downstream Ehrlich module *ylARO10-ylARO8-GapY3-PAR3* was integrated at the genome pBR docking site of **pol1fk1**, obtaining strain **pol1fk1P**. Although shake flask cultivation of **pol1fk1P** showed no improvement in 2-PE titer, the byproduct phenylacetate was significantly decreased to 124.49 mg/L (Figure 5b, 532.48 mg/L phenylacetate in **polgP8-6**).

In addition, prephenate dehydratase PHA2 catalyzes the anaplerotic reaction from phenylpyruvate to prephenate (Figure 1). Deletion of gene *PHA2* in strain **pol1fk1** generated strain **pol1fk2**. Chromosomally integrated (integrated at pBR docking site) Ehrlich module (*ylARO10-ylARO8-GapY3-PAR3*) in **pol1fk2** (strain **pol1fk2P**) leads to an improved 2-PE titer of 1809.65 mg/L with the yield at 0.570 g/g_{L-phenylalanine} compared to **pol1fk1P** (Figure 5b,c, 1735.78 mg/L with yield at 0.550 g/g_{L-phenylalanine}), but a significant decrease in biomass was observed in **pol1fk2P** (Figure 5a). On the other hand, 4-hydroxyphenylpyruvate dioxygenase (encoded by gene *ylHPD*) could convert phenylpyruvate to 2-hydroxyphenylacetate. Therefore, we further knocked out *ylHPD* in strain **pol1fk2**, obtaining strain **pol1fk3**. However, the chromosomally integrated (integrated at pBR docking site) Ehrlich module in **pol1fk3** (strain **pol1fk3P**) leads to decreased 2-PE production and increased phenylacetate titer, which were 1432.43 and 226.17 mg/L (Figure 5b), respectively. This result suggests that *ylHPD* cannot be knocked out in this scenario. It is not clear why the deletion of gene *ylHPD* has a negative result, possibly due to the incorrect annotation of the reaction directionality of *ylHPD*.

We have refactored the Ehrlich pathway and blocked the byproducts synthesis, and integrated the optimal gene module *ylARO10-ylARO8-GapY3-PAR3* to the pBR docking site of the triple knockout strain (**pol1fk2**, *ALD2*, *ALD3*, and *PHA2* were knocked out). In previous work, our group has established a 26s rDNA/Cre-loxP-based iterative gene integration and marker-curation method.³⁶ With more than 200 copies of ribosome DNAs in *Y. lipolytica*, this technique allows genes of interests to be randomly integrated into the genome with multiple copies. Thus, we next sought to apply this method and further optimize the Ehrlich pathway, including genes *ylARO10*, *ylARO8*, *GapY3*, and *PAR4*. To obtain a productive

strain, we screened 144 genome-integrated transformants by 24-well deep plate cultivation in glucose-YNB medium with 4 g/L L-phenylalanine (Figure 5d). About 45% of the genome-integrated produced 2-PE at 900–1000 mg/L, less than 5% of the screened strain produced 2-PE over 1200 mg/L. Then the top-performed strains were further validated in shake flasks (Figure 5e,f). Strain **pol1fk4-2** produced the highest 2-PE of 1817.46 mg/L with the yield at 0.590 g/g_{L-phenylalanine}.

A Nonnative 2-Oxoglutarate (aKG) Shuttle to Improve Metabolite Trafficking.

As suggested by the mathematical model (Supplementary Note S1), we next sought to improve the precursor (2-oxoglutarate, aKG) flux. Noteworthy, *Y. lipolytica* is known for the strong TCA metabolic activity.³⁷ Indeed, we detected 4.84 g/L of citrate at 72 h of cultivation in strain **pol1fk4-2** (Figure 6b). Thus, rewiring the overflowed citrate flux to cytosolic aKG is a

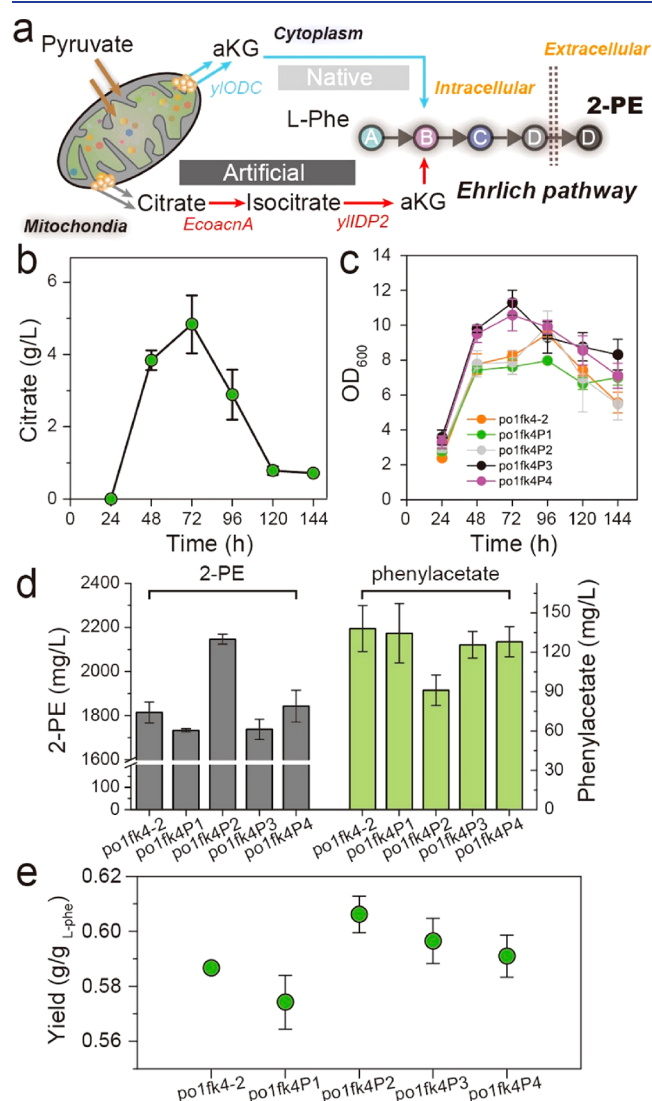


Figure 6. Overcoming cellular compartmentalization of 2-oxoglutarate (aKG) to increase aKG availability. (a) Construction of cytosolic source for 2-oxoglutarate synthesis by coupling bacterial aconitase with the overflowed citrate from Krebs cycle. (b) Citrate titers of strain **pol1fk4-2**. (c–e) 2-PE titers, cell growth and yield of strains **pol1fk4P1**, **pol1fk4P2**, **pol1fk4P3**, and **pol1fk4P4**. All experiments were performed in triplicate and error bars show standard deviation (SD).

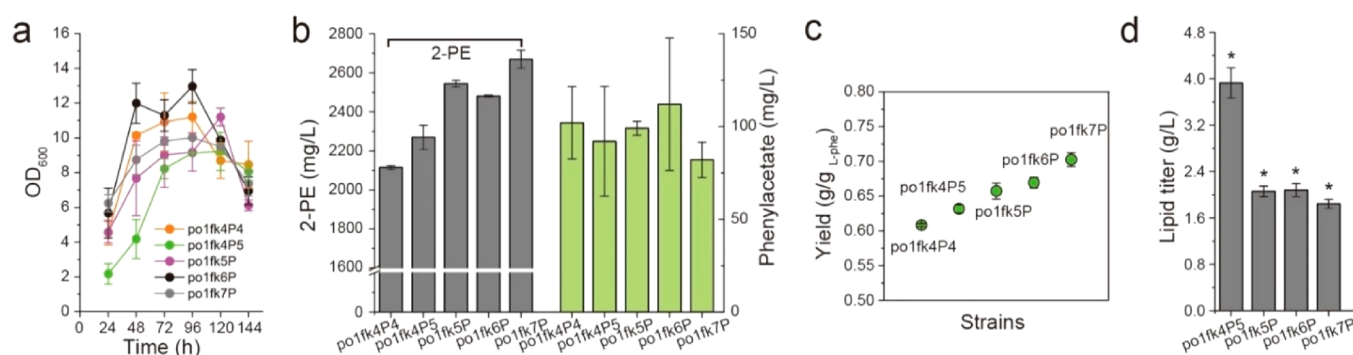


Figure 7. Improving 2-oxoglutarate trafficking across the mitochondria membrane by overexpressing the mitochondrial 2-oxodicarboxylate carrier yIODC1 and improving 2-PE titer by blocking fatty acid synthesis. (a–d) 2-PE titers, cell growth, yield, and lipid titers of strains **po1fk4P5**, **po1fk5P**, **po1fk6P**, and **po1fk7P**. All experiments were performed in triplicate and error bars show standard deviation (SD). The * indicates $p < 0.01$ (two-tailed test).

feasible strategy to increase precursor (aKG) supply and improve 2-PE production. Nevertheless, *Y. lipolytica* lacks the cytosolic aconitate hydratase and isocitrate dehydrogenase. To construct the cytosolic pathway from citrate to aKG (Figure 6a), we introduced two aconitate hydratases, including CitB from *Bacillus subtilis* and AcnA from *E. coli*, and a cytosolic isocitrate dehydrogenase ScIDP2 from *S. cerevisiae*.³⁸ Additionally, by searching the genome of *Y. lipolytica* with ScIDP2 as template, we retrieved a putative cytosolic isocitrate dehydrogenase yIDP2 (encoded by gene *YALIOF04095g*). Subsequently, four nonnative aKG source pathways, including *citB-scIDP2*, *citB-yIDP2*, *acnA-scIDP2*, and *acnA-yIDP2*, were introduced into **po1fk4–2** by plasmid pYLXP'. The resulting strains **po1fk4P1**, **po1fk4P2**, **po1fk4P3**, and **po1fk4P4** produced 1733.45, 2146.45, 1737.58, and 1842.85 mg/L of 2-PE with yield of 0.574, 0.606, 0.597, and 0.591 g/g_{L-phenylalanine} in shake flasks (Figure 6c,d,e), respectively. It indicates the coexpression of *citB* and *yIDP2* could effectively convert cytosolic citrate to aKG. In addition, we also overexpressed the mitochondrial 2-oxodicarboxylate carrier yIODC1 (encoded by gene *YALIOD02629g*) to export 2-oxoglutarate (aKG) out of the mitochondrial matrix to the cytosol (strain **po1fk4P5**, **po1fk4–2** harboring plasmid pYLXP'-*citB-yIDP2-yIODC*). As expected, the 2-PE titer and yield in **po1fk4P5** were further increased, reaching 2269.08 mg/L and 0.632 g/g_{L-phenylalanine} (Figure 7a,b,c), respectively.

On the other hand, *Y. lipolytica* is known to accumulate up to 30–60% dry cell weight as lipid.^{10,39} As shown in Figure 1b, production of 1 mol of fatty acids (stearic acids C18:0) will consume 16 mol of NADPH and 9 mol of citrate (acetyl-CoA). As a result, the synthesis of lipid competes with aconitase (aconitate hydratases) and PARs for cytosolic citrate and NADPH. Specially, diacylglycerol acyltransferases have been identified as the rate-limiting steps to lipid synthesis via the Kennedy pathway in *Y. lipolytica*.^{40,41} Thus, we pursued further to knock out the diacylglycerol acyltransferases, encoded by *yIDGA1* (*YALIOE32769g*) and *yIDGA2* (*YALIOD07986g*), to mitigate fatty acid synthesis. Shake flask cultivation of the resulting strain **po1fk5P** (**po1fk4–2** $\Delta yIDGA1::loxP$ harboring pYLXP'-*citB-yIDP2-yIODC*), **po1fk6P** (**po1fk4–2** $\Delta yIDGA2::loxP$ harboring pYLXP'-*citB-yIDP2-yIODC*), and **po1fk7P** (**po1fk4–2** $\Delta yIDGA1::loxP$ $\Delta yIDGA2::loxP$ harboring pYLXP'-*citB-yIDP2-yIODC*) all led to significant improvements in 2-PE titers and yield (Figure 7a,b,c). Specifically, strain **po1fk7P** produced 2669.54 mg/L of

2-PE with yield at 0.702 g/g_{L-phenylalanine} (Figure 7a,b,c), which was 1.11-fold and 1.18-fold higher than strain **po1fk4P5**. Furthermore, to validate the impacts of *yIDGA1* and *yIDGA2* deletion on lipid production, we measured the lipid titer in strains **po1fk4P5**, **po1fk5P**, **po1fk6P**, and **po1fk7P** (Figure 7d), reaching 3.93, 2.06, 2.08, and 1.84 g/L, respectively. These results confirmed that fatty acid synthesis was indeed mitigated by deleting genes *yIDGA1* and *yIDGA2*. In conclusion, by constructing a cytosolic aKG pathway and expression of the dicarboxylic acid transporter (yIODC) as well as mitigating fatty acids synthesis, we efficiently improved the aKG flux and 2-PE tier and yield.

CONCLUSIONS

Efficient microbial synthesis of chemicals necessitates systematic debottlenecking, refactoring and optimization of the native or nonnative metabolic pathways. With 2-PE as a tested molecule, we analyzed the stoichiometric constraints of the Ehrlich pathway toward efficient synthesis of the target molecules in *Y. lipolytica*. The proposed metabolic model reveals potential engineering targets for high yield production of 2-PE with cosubstrate feeding of glucose and L-phenylalanine. Specifically, guided by the model, we identified that the catalytic efficiency of the Ehrlich pathway and the precursor 2-oxoglutarate (aKG) supplement might be the rate-limiting steps. Stepwise refactoring the Ehrlich pathway and overcoming the cellular compartmentalization of precursor (aKG) significantly improved 2-PE production. By blocking the precursor-competing pathways and mitigating fatty acids synthesis, the engineered strain produced 2669.54 mg/L of 2-PE with yield at 0.702 g/g in shake flasks, which were 4.16 and 2.07-fold of the starting strain, respectively. The strategies reported in this study should be adding value and guide us to engineer other complex metabolic pathways for various biomanufacturing applications.

Further investigations on relieving 2-PE toxicity and promoting cell fitness are viable solutions to improve 2-PE production. Major considerations should include 2-PE tolerance/toxicity, medium composition, and optimal fermentation processes. In general, mutagenesis coupled with high throughput screening is an efficient and convenient way to evolve tolerance phenotype.⁴² In addition, small amounts of organic nitrogen sources, such as peptone and yeast extract, benefit cell growth without inhibiting the Ehrlich pathway.⁴³ Moreover, it was found that both Ca^{2+} and Mg^{2+} salts protect

the cell and facilitate 2-PE production by increasing membrane stability and integrity.⁴⁴ Besides, by adding organic solvents as overlays during fermentation, 2-PE titer could be increased to 12.6 g/L in the concentrated organic layer.⁴⁵ These strategies will enable us to build a sustainable 2-PE platform at low cost and high efficiency.

MATERIALS AND METHODS

Strains, Plasmid, Primers, and Chemicals. All strains of engineered *Y. lipolytica*, including the genotypes of manipulations, recombinant plasmids, and primers, have been listed in [Supplementary Table S1 and S2](#). Chemicals used in this study include phenylacetaldehyde, L-phenylalanine, phenylacetate, 2-phenylethanol, 2-oxoglutarate, and citrate, which were all purchased from Sigma-Aldrich.

Shake Flask and 24-Well Deep-Plate Cultivations. All engineered strains were underwent optimal screening before shake flask cultivations (see [Yeast Transformation and Screening of High-Producing Strains, Figure 3a](#)). For shake flask cultivations, seed culture was carried out in the shaking tube with 2 mL seed culture medium at 30 °C and 250 r.p.m. for 48 h. Then, 0.8 mL of seed culture was inoculated into the 250 mL flask containing 35 mL of fermentation medium and grown under the conditions of 30 °C and 250 r.p.m. for 144 h. One milliliter of cell suspension was sampled every 24 h for OD₆₀₀, glucose, 2-PE, L-phenylalanine, and phenylacetate measurements. For performing 24-well deep-plate cultivation, engineered *Y. lipolytica* strains were first cultured in 96-wells plates with 150 μ L seed culture medium at 30 °C and 1000 r.p.m. for 36 h. Sequentially, 40 μ L of seed culture was inoculated to the 24-well deep plate with 2 mL fermentation medium at 30 °C and 1000 r.p.m. for 96 h, and finally, 1 mL of cell suspension was sampled for 2-PE, L-phenylalanine, and phenylacetate measurements.

The seed culture medium used in this study was the yeast complete synthetic media regular media CSM containing the following: glucose 20.0 g/L, yeast nitrogen base (without ammonium sulfate) 1.7 g/L, ammonium sulfate 5.0 g/L, and CSM-Leu or CSM-Ura 0.74 g/L. Two types of fermentation medium were used in our work, including nitrogen-limited media CSM and YNB. The nitrogen-limited media CSM contained the following: glucose 40.0 g/L, yeast nitrogen base (without ammonium sulfate) 1.7 g/L, ammonium sulfate 1.1 g/L, CSM-Leu 0.74 g/L, and appropriate L-phenylalanine. The nitrogen-limited media YNB contained the following: glucose 40.0 g/L, yeast nitrogen base (without ammonium sulfate) 1.7 g/L, leucine or uracil 0.2 g/L, and appropriate L-phenylalanine.

Whole-Cell Bioconversion of Phenylacetaldehyde. To prepare the whole-cell biocatalyst, cells were harvested during the exponential growth phase (48 h) from the shake flask cultivation. Then, cells were washed twice with 100 mM phosphate buffer (pH 7.0), and resuspended to an OD₆₀₀ of 4 in the same buffer. Next, whole-cell biocatalytic conversion of phenylacetaldehyde was performed in 20-mL glass tube containing 1 mL of cell suspension (OD₆₀₀ = 4) and 1 mL phenylacetaldehyde–water solution (2 g/L phenylacetaldehyde) at 30 °C and 250 r.p.m. for 4 h. One hundred microliters of cell suspension was sampled every 1 h for 2-PE and phenylacetate measurements.

Yeast Transformation and Screening of High-Producing Strains. The standard protocols of *Y. lipolytica* transformation by the lithium acetate method were described as previously reported.^{36,46} In brief, 1 mL of cells was harvested

during the exponential growth phase (16–24 h) from 2 mL YPD medium (yeast extract 10 g/L, peptone 20 g/L, and glucose 20 g/L) in the 14 mL shake tube, and washed twice with 100 mM phosphate buffer (pH 7.0). Then, cells were resuspended in 105 μ L transformation solution, containing 90 μ L 50% PEG4000, 5 μ L lithium acetate (2 M), 5 μ L boiled single stand DNA (salmon sperm, denatured), and 5 μ L DNA products (including 200–500 ng of plasmids, linear plasmids or DNA fragments), and incubated at 39 °C for 1 h, then spread on selected plates. It should be noted that the transformation mixtures needed to be vortexed for 15 s every 15 min during the process of 39 °C incubation. The selected markers, including leucine and uracil, were used in this study. All engineering strains after genetic manipulations were performed optimized screening by the shaking tube cultivations, and the optimal strain was used to perform shaking flask (these data have been shown in [Supporting Information](#)).

Expression Vectors Construction and Pathway Assembly. The YaliBrick plasmid pYLXP' was used as the expression vector in this study.^{47,48} Plasmid constructions were performed by using previously described methods.^{36,49} In brief, recombinant plasmids of pYLXP'-XX (a single gene expression) were obtained by Gibson Assembly method⁵⁰ using linearized pYLXP' (digested by *SnaBI* and *KpnI*) and the appropriate PCR-amplified DNA fragment. Multigenes assembly was achieved by restriction enzyme digestion subcloning based on the application of isocaudamers *AvrII* and *NheI*.^{47,51} All genes were respectively expressed by the TEF promoter with intron sequence and XPR terminator. The modified DNA fragments and plasmids were sequenced by Quintarbio. The endonucleases used in this research were purchased from Thermo Fisher Scientific or NEB.

Gene Knockout and 26s rDNA Genomic Integration of Ehrlich Pathway. A marker-free gene knockout method based on Cre-*lox* recombination system was used as previously reported.⁵² For performing gene knockout, the upstream and downstream sequences (both 1000 bp) flanking the deletion targets were PCR-amplified. These two fragments, the *loxP*-*URA-loxP* cassette (digested from plasmid pYLXP'-*loxP*-*URA* by *AvrII* and *SalI*), and the residual plasmid backbone of pYLXP'-*loxP*-*URA* were joined by the Gibson Assembly method, obtaining the gene knockout plasmids pYLXP'-*loxP*-*URA*-XX. The obtained plasmids were sequenced by Quintarbio. Next, the gene knockout cassettes were PCR-amplified from construction plasmids pYLXP'-*loxP*-*URA*-XX, and further transformed into *Y. lipolytica*. The positive transformants were determined by colony PCR. Next, plasmid pYLXP'-*Cre* was introduced into the positive transformants and promoted the recombination of *loxP* sites, which recycle the selected marker. Finally, the intracellular plasmid pYLXP'-*Cre* was evicted by incubation at 30 °C for 48 h.

The standard protocol of 26s rDNA genomic integration also has been described in previous reported.³⁶ For 26s rDNA genomic integration of the Ehrlich pathway, the expression plasmid pYLXP'-*ylARO10-ylARO8-GapY3-PAR4* was digested by *AvrII* and *NotI*, and the fragment containing the Ehrlich pathway was inserted into linearized pYLXP'-*loxP*-*URA* digested by *NheI* and *NotI*, getting pYLXP'-*loxP*-*URA-ylARO10-ylARO8-GapY3-PAR4*. The homologous arms of 26s rDNA, including 26s rDNA 1s and 2s, were PCR-amplified by appropriate primers. And next, these two homologous-arm fragments, Ehrlich pathway with the *loxP*-*URA-loxP* cassette (digested from plasmid pYLXP'-*loxP*-*URA-ylARO10-ylARO8*-

GapY3-PAR4 by *AvrII* and *NotI*), and the residual plasmid backbone of pYLXP'-*loxP*-URA-*ylARO10-ylARO8-GapY3-PAR4* were joined by Gibson Assembly method, obtaining the 26s rDNA genomic integration plasmids prDNAloxP-*ylARO10-ylARO8-GapY3-PAR4*. Then, the 26s rDNA genomic integration cassette of the Ehrlich pathway was gotten by digesting prDNAloxP-*ylARO10-ylARO8-GapY3-PAR4* with *AvrII* and *NotI*, and the integration cassette was further transformed into *Y. lipolytica*. In addition, the manipulation of recycling the selected marker was similar to gene knockout.

Quantification of Cell Density, 2-PE, Penylacetate, L-Phenylalanine, Glucose, Citrate, Fatty Acid, and Y_{2-PE} Calculation. Cell densities were monitored by measuring the optical density at 600 nm (OD₆₀₀). The concentrations of 2-PE, penylacetate, and L-phenylalanine were measured by high-performance liquid chromatography (HPLC) through Agilent HPLC 1220 equipped with a ZORBAX Eclipse Plus C18 column (4.6 × 100 mm, 3.5 μm, Agilent) and a VWD detector. The analysis was performed at 215 nm under 40 °C column temperature with a mobile phase comprising 50% (v/v) methanol in water at a flow rate of 0.5 mL/min. The concentrations of glucose and citrate were also measured by Agilent HPLC 1220 equipped with a Supelcogel Carbohydrate column (Sigma, USA) and a refractive index detector. H₂SO₄ (5 mM) was used as the mobile phase at a flow rate of 0.6 mL/min at 40 °C. The method of quantification of fatty acid was used as previously reported.³⁹ Y_{2-PE} is the 2-PE yield relative to the consumption of L-phenylalanine.

■ ASSOCIATED CONTENT

Supporting Information

The Supporting Information is available free of charge at <https://pubs.acs.org/doi/10.1021/acssynbio.9b00468>.

Supplementary Table S1. Strains and plasmids; Supplementary Table S2. Primers and Oligos; Supplementary Table S3. Strain performance; Supplementary Note. Stoichiometric model to assess Ehrlich pathway efficiency; Supplementary Figure S1. Stoichiometric models reveal that 2-PE yield is driven by selectivity of the Ehrlich pathway and supply of 2-oxoglutarate (aKG); Supplementary Figure S2. 2-PE titers of screening L-phenylalanine specific permeases with the addition of final concentration of 4g/L L-phenylalanine into CSM fermentation medium (48 h) in shake cultivations; Supplementary Figure S3. 2-PE titers of strain strains polgP7-1, polgP7-2, polgP7-3, polgP7-4, polgP7-5, and polgP7-6 in shake cultivations (PDF)

■ AUTHOR INFORMATION

Corresponding Author

Peng Xu – Department of Chemical, Biochemical and Environmental Engineering, University of Maryland, Baltimore County, Baltimore, Maryland 21250, United States; orcid.org/0000-0002-0999-8546; Email: pengxu@umbc.edu

Authors

Yang Gu – Department of Chemical, Biochemical and Environmental Engineering, University of Maryland, Baltimore County, Baltimore, Maryland 21250, United States; Key Laboratory of Carbohydrate Chemistry and Biotechnology,

Ministry of Education, Jiangnan University, Wuxi 214122, China

Jingbo Ma – Department of Chemical, Biochemical and Environmental Engineering, University of Maryland, Baltimore County, Baltimore, Maryland 21250, United States

Yonglian Zhu – Key Laboratory of Carbohydrate Chemistry and Biotechnology, Ministry of Education, Jiangnan University, Wuxi 214122, China

Complete contact information is available at:

<https://pubs.acs.org/10.1021/acssynbio.9b00468>

Author Contributions

PX and YG conceived the topic. YG developed the models, performed genetic engineering and fermentation experiments with input from JM and YZ. YG and PX wrote the manuscript.

Notes

The authors declare no competing financial interest.

■ ACKNOWLEDGMENTS

This work was supported by the Cellular & Biochemical Engineering Program of the National Science Foundation under grant no. 1805139 and the Bill & Melinda Gates Foundation under grant no. OPP1188443. YG would like to thank the School of Biotechnology in Jiangnan University for funding support.

■ REFERENCES

- (1) Nielsen, J., and Keasling, J. D. (2016) Engineering Cellular Metabolism. *Cell* 164, 1185–1197.
- (2) Luo, X., Reiter, M. A., d'Espaux, L., Wong, J., Denby, C. M., Lechner, A., Zhang, Y., Grzybowski, A. T., Harth, S., Lin, W., Lee, H., Yu, C., Shin, J., Deng, K., Benites, V. T., Wang, G., Baidoo, E. E. K., Chen, Y., Dev, I., Petzold, C. J., and Keasling, J. D. (2019) Complete biosynthesis of cannabinoids and their unnatural analogues in yeast. *Nature* 567, 123–126.
- (3) Westfall, P. J., Pitera, D. J., Lenihan, J. R., Eng, D., Woolard, F. X., Regentin, R., Horning, T., Tsuruta, H., Melis, D. J., Owens, A., Fickes, S., Diola, D., Benjamin, K. R., Keasling, J. D., Leavell, M. D., McPhee, D. J., Renninger, N. S., Newman, J. D., and Paddon, C. J. (2012) Production of amorphadiene in yeast, and its conversion to dihydroartemisinic acid, precursor to the antimalarial agent artemisinin. *Proc. Natl. Acad. Sci. U. S. A.* 109, E111–E118.
- (4) Ajikumar, P. K., Xiao, W. H., Tyo, K. E., Wang, Y., Simeon, F., Leonard, E., et al. (2010) Isoprenoid pathway optimization for taxol precursor overproduction in *Escherichia coli*. *Science* 330, 70–74.
- (5) Li, J., Mutanda, I., Wang, K., Yang, L., Wang, J., and Wang, Y. (2019) Chloroplastic metabolic engineering coupled with isoprenoid pool enhancement for committed taxanes biosynthesis in *Nicotiana benthamiana*. *Nat. Commun.* 10, 4850.
- (6) Atsumi, S., Hanai, T., and Liao, J. C. (2008) Non-fermentative pathways for synthesis of branched-chain higher alcohols as biofuels. *Nature* 451, 86–89.
- (7) Zhang, K., Sawaya, M., Eisenberg, D., and Liao, J. (2008) Expanding metabolism for biosynthesis of nonnatural alcohols. *Proc. Natl. Acad. Sci. U. S. A.* 105, 20653–20658.
- (8) Qin, J., Zhou, Y. J., Krivoruchko, A., Huang, M., Liu, L., Khoomrung, S., Siewers, V., Jiang, B., and Nielsen, J. (2015) Modular pathway rewiring of *Saccharomyces cerevisiae* enables high-level production of L-ornithine. *Nat. Commun.* 6, 8224.
- (9) Park, S. H., Kim, H. U., Kim, T. Y., Park, J. S., Kim, S. S., and Lee, S. Y. (2018) Metabolic engineering of *Corynebacterium glutamicum* for L-arginine production. *Nat. Commun.* 5, 4618.
- (10) Xu, P., Gu, Q., Wang, W. Y., Wong, L., Bower, A. G. W., Collins, C. H., and Koffas, M. A. G. (2013) Modular optimization of multi-gene pathways for fatty acids production in *E. coli*. *Nat. Commun.* 4, 8.

- (11) Xu, P., Qiao, K., Ahn, W. S., and Stephanopoulos, G. (2016) Engineering *Yarrowia lipolytica* as a platform for synthesis of drop-in transportation fuels and oleochemicals. *Proc. Natl. Acad. Sci. U. S. A.* 113, 10848–10853.
- (12) Xu, P., Qiao, K., and Stephanopoulos, G. (2017) Engineering oxidative stress defense pathways to build a robust lipid production platform in *Yarrowia lipolytica*. *Biotechnol. Bioeng.* 114, 1521–1530.
- (13) Price, J. V., Chen, L., Whitaker, W. B., Papoutsakis, E., and Chen, W. (2016) Scaffoldless engineered enzyme assembly for enhanced methanol utilization. *Proc. Natl. Acad. Sci. U. S. A.* 113, 12691–12696.
- (14) Gu, Y., Lv, X., Liu, Y., Li, J., Du, G., Chen, J., Rodrigo, L.-A., and Liu, L. (2019) Synthetic redesign of central carbon and redox metabolism for high yield production of N-acetylglucosamine in *Bacillus subtilis*. *Metab. Eng.* 51, 59–69.
- (15) Xu, P., Bhan, N., and Koffas, M. A. G. (2013) Engineering plant metabolism into microbes: from systems biology to synthetic biology. *Curr. Opin. Biotechnol.* 24, 291–299.
- (16) Xu, P. (2018) Production of chemicals using dynamic control of metabolic fluxes. *Curr. Opin. Biotechnol.* 53, 12–19.
- (17) Gupta, A., Reizman, I. M. B., Reisch, C. R., and Prather, K. L. J. (2017) Dynamic regulation of metabolic flux in engineered bacteria using a pathway-independent quorum-sensing circuit. *Nat. Biotechnol.* 35, 273–279.
- (18) Doong, S. J., Gupta, A., and Prather, K. L. J. (2018) Layered dynamic regulation for improving metabolic pathway productivity in *Escherichia coli*. *Proc. Natl. Acad. Sci. U. S. A.* 115, 2964–2969.
- (19) Xiao, Y., Bowen, C. H., Liu, D., and Zhang, F. (2016) Exploiting nongenetic cell-to-cell variation for enhanced biosynthesis. *Nat. Chem. Biol.* 12, 339–344.
- (20) Wang, M., Chen, B., Fang, Y., and Tan, T. (2017) Cofactor engineering for more efficient production of chemicals and biofuels. *Biotechnol. Adv.* 35, 1032–1039.
- (21) Wu, G., Yan, Q., Jones, J. A., Tang, Y. J., Fong, S. S., and Koffas, M. A. G. (2016) Metabolic Burden: Cornerstones in Synthetic Biology and Metabolic Engineering Applications. *Trends Biotechnol.* 34, 652–664.
- (22) Dueber, J. E., Wu, G. C., Malmirchegini, G. R., Moon, T. S., Petzold, C. J., Ullal, A. V., Prather, K. L. J., and Keasling, J. D. (2009) Synthetic protein scaffolds provide modular control over metabolic flux. *Nat. Biotechnol.* 27, 753–759.
- (23) Delebecque, C. J., Lindner, A. B., Silver, P. A., and Aldaye, F. A. (2011) Organization of Intracellular Reactions with Rationally Designed RNA Assemblies. *Science* 333, 470–474.
- (24) Park, J. O., Liu, N., Holinski, K. M., Emerson, D. F., Qiao, K., Woolston, B. M., Xu, J., Lazar, Z., Islam, M. A., Vidoudez, C., Girguis, P. R., and Stephanopoulos, G. (2019) Synergistic substrate cofeeding stimulates reductive metabolism. *Nat. Metab.* 1, 643–651.
- (25) Lv, Y., Qian, S., Du, G., Chen, J., Zhou, J., and Xu, P. (2019) Coupling feedback genetic circuits with growth phenotype for dynamic population control and intelligent bioproduction. *Metab. Eng.* 54, 109–116.
- (26) Liu, N., Santala, S., and Stephanopoulos, G. (2020) Mixed carbon substrates: a necessary nuisance or a missed opportunity? *Curr. Opin. Biotechnol.* 62, 15–21.
- (27) Liu, H., Marsafari, M., Wang, F., Deng, L., and Xu, P. (2019) Engineering acetyl-CoA metabolic shortcut for eco-friendly production of polyketides triacetic acid lactone in *Yarrowia lipolytica*. *Metab. Eng.* 56, 60–68.
- (28) Liu, C., Zhang, K., Cao, W., Zhang, G., Chen, G., Yang, H., Wang, Q., Liu, H., Xian, M., and Zhang, H. (2018) Genome mining of 2-phenylethanol biosynthetic genes from *Enterobacter* sp. CGMCC 5087 and heterologous overproduction in *Escherichia coli*. *Biotechnol. Biofuels* 11, 305.
- (29) Qian, X., Yan, W., Zhang, W., Dong, W., Ma, J., Ochsenreither, K., Jiang, M., and Xin, F. (2019) Current status and perspectives of 2-phenylethanol production through biological processes. *Crit. Rev. Biotechnol.* 39, 235–248.
- (30) Yang, Z., Edwards, H., and Xu, P. (2020) CRISPR-Cas12a/Cpf1-assisted precise, efficient and multiplexed genome-editing in *Yarrowia lipolytica*. *Metab. Eng. Commun.* 10, No. e00112.
- (31) Abdel-Mawgoud, A. M., Markham, K. A., Palmer, C. M., Liu, N., Stephanopoulos, G., and Alper, H. S. (2018) Metabolic engineering in the host *Yarrowia lipolytica*. *Metab. Eng.* 50, 192–208.
- (32) Groenewald, M., Boekhout, T., Neuvéglise, C., Gaillardin, C., van Dijk, P. W. M., and Wyss, M. (2014) *Yarrowia lipolytica*: Safety assessment of an oleaginous yeast with a great industrial potential. *Crit. Rev. Microbiol.* 40, 187–206.
- (33) Martinez-Avila, O., Sanchez, A., Font, X., and Barrena, R. (2018) Bioprocesses for 2-phenylethanol and 2-phenylethyl acetate production: current state and perspectives. *Appl. Microbiol. Biotechnol.* 102, 9991–10004.
- (34) Wang, Z., Jiang, M., Guo, X., Liu, Z., and He, X. (2018) Reconstruction of metabolic module with improved promoter strength increases the productivity of 2-phenylethanol in *Saccharomyces cerevisiae*. *Microb. Cell Fact.* 17, 60.
- (35) Ruiz, S. J., van't Klooster, J. S., Bianchi, F., and Poolman, B. (2017) Growth inhibition by amino acids in *Saccharomyces cerevisiae*. *bioRxiv*, 2017, 222224. DOI: 10.1101/222224, accessed 2017/12/01.
- (36) Lv, Y., Edwards, H., Zhou, J., and Xu, P. (2019) Combining 26s rDNA and the Cre-loxP System for Iterative Gene Integration and Efficient Marker Curation in *Yarrowia lipolytica*. *ACS Synth. Biol.* 8, 568–576.
- (37) Markham, K. A., and Alper, H. S. (2018) Synthetic Biology Expands the Industrial Potential of *Yarrowia lipolytica*. *Trends Biotechnol.* 36, 1085–1095.
- (38) Bojunga, N., and Entian, K. D. (1999) Cat8p, the activator of gluconeogenic genes in *Saccharomyces cerevisiae*, regulates carbon source-dependent expression of NADP-dependent cytosolic isocitrate dehydrogenase (Idp2p) and lactate permease (Jen1p). *Mol. Gen. Genet.* 262, 869–875.
- (39) Xu, P., Li, L. Y., Zhang, F. M., Stephanopoulos, G., and Koffas, M. (2014) Improving fatty acids production by engineering dynamic pathway regulation and metabolic control. *Proc. Natl. Acad. Sci. U. S. A.* 111, 11299–11304.
- (40) Beopoulos, A., Haddouche, R., Kabran, P., Dulermo, T., Chardot, T., and Nicaud, J. M. (2012) Identification and characterization of DGA2, an acyltransferase of the DGAT1 acyl-CoA:diacylglycerol acyltransferase family in the oleaginous yeast *Yarrowia lipolytica*. New insights into the storage lipid metabolism of oleaginous yeasts. *Appl. Microbiol. Biotechnol.* 93, 1523–37.
- (41) Gajdos, P., Ledesma-Amaro, R., Nicaud, J. M., Certik, M., and Rossignol, T. (2016) Overexpression of diacylglycerol acyltransferase in *Yarrowia lipolytica* affects lipid body size, number and distribution. *FEMS Yeast Res.* 16, fow062.
- (42) Wang, Y., Zhang, H., Lu, X., Zong, H., and Zhuge, B. (2019) Advances in 2-phenylethanol production from engineered microorganisms. *Biotechnol. Adv.* 37, 403–409.
- (43) Cui, Z., Yang, X., Shen, Q., Wang, K., and Zhu, T. (2011) Optimisation of biotransformation conditions for production of 2-phenylethanol by a *Saccharomyces cerevisiae* CWY132 mutant. *Nat. Prod. Res.* 25, 754–759.
- (44) Ciesarova, Z., Smogrovicova, D., and Domy, Z. (1996) Enhancement of yeast ethanol tolerance by calcium and magnesium. *Folia Microbiol.* 41, 485–8.
- (45) Stark, D., Munch, T., Sonleitner, B., Marison, I. W., and von Stockar, U. (2002) Extractive bioconversion of 2-phenylethanol from L-phenylalanine by *Saccharomyces cerevisiae*. *Biotechnol. Prog.* 18, 514–23.
- (46) Lv, Y., Marsafari, M., Koffas, M., Zhou, J., and Xu, P. (2019) Optimizing Oleaginous Yeast Cell Factories for Flavonoids and Hydroxylated Flavonoids Biosynthesis. *ACS Synth. Biol.* 8, 2514–2523.
- (47) Wong, L., Engel, J., Jin, E., Holdridge, B., and Xu, P. (2017) YaliBricks, a versatile genetic toolkit for streamlined and rapid pathway engineering in *Yarrowia lipolytica*. *Metab. Eng. Commun.* 5, 68–77.

(48) Wong, L., Holdridge, B., Engel, J., and Xu, P. (2019) Genetic Tools for Streamlined and Accelerated Pathway Engineering in *Yarrowia lipolytica*. In *Microbial Metabolic Engineering: Methods and Protocols* (Santos, C. N. S., and Ajikumar, P. K., Eds.) pp 155–177, Springer, New York, NY.

(49) Marsafari, M., and Xu, P. (2020) Debottlenecking mevalonate pathway for antimalarial drug precursor amorpha-4,11-diene biosynthesis in *Yarrowia lipolytica*. *Metab. Eng. Commun.* 10, No. e00121.

(50) Gibson, D. G., Young, L., Chuang, R.-Y., Venter, J. C., Hutchison, C. A., III, and Smith, H. O. (2009) Enzymatic assembly of DNA molecules up to several hundred kilobases. *Nat. Methods* 6, 343–345.

(51) Xu, P., Vansiri, A., Bhan, N., and Koffas, M. (2012) ePathBrick: A Synthetic Biology Platform for Engineering Metabolic Pathways in *E. coli*. *ACS Synth. Biol.* 1, 256–266.

(52) Fickers, P., Le Dall, M. T., Gaillardin, C., Thonart, P., and Nicaud, J. M. (2003) New disruption cassettes for rapid gene disruption and marker rescue in the yeast *Yarrowia lipolytica*. *J. Microbiol. Methods* 55, 727–737.